JOURNAL OF GEOPHYSICAL RESEARCH, VOL. 92, NO. B12, PAGES 12,846–12,856, NOVEMBER 10, 1987

# A New Reduction Algorithm for Marine Heat Flow Measurements

HEINER VILLINGER[1] AND EARL E. DAVIS

*Pacific Geoscience Centre, Geological Survey of Canada, Sidney, British Columbia*

Multiple penetration heat flow surveys that employ "violin bow" multithermistor array instruments generate large quantities of high-quality data. To cope with the problems associated with the reduction of these data, an algorithm has been developed which can be used to reduce the data automatically on a microcomputer. The algorithm is designed for use with a pulsed line source method of conductivity measurement, although it could be modified easily for use with the continuous line source method. The multiply iterative algorithm deals, on a sensor by sensor basis, with errors associated with nonideal probe construction and sediment entry, factors that affect the determination of both in situ temperatures and thermal conductivities. Numerical tests of the algorithm show that it is accurate and stable and fast enough for post-real-time reduction of data at sea. Practical tests on high-quality data from the western Pacific show that accuracies are limited by the instrumental resolution; in these cases, the reduction algorithm provided determinations of undisturbed in situ temperatures to better than 1 mK and of in situ conductivities to within 1%.

## INTRODUCTION

Most contemporary marine heat flow studies have a common requirement for high accuracy. Obvious examples include those carried out to determine better the characteristic relationship between heat flow and lithospheric age (e.g., *Davis et al.*, 1984; *Louden et al.*, 1987], to estimate seafloor age from heat flow in the absence of other more directly applicable information [e.g., *Langseth et al.*, 1980; *Tamaki*, 1985], and to establish the anomalous heat flow associated with major hot spots [e.g., *Von Herzen et al.*, 1982; *Detrick et al.*, 1986; *Courtney and White*, 1986]. Others include studies in ridge crest and back arc environments, where heat flow variability can provide information about the nature of hydrothermal circulation in the crust beneath the mantle of sediment through which the heat flow is determined [e.g., *Green et al.*, 1981; E. E. Davis and H. Villinger, manuscript in preparation, 1987], and where the determination of any nonconductive component of heat flow may provide information about the rate of pore fluid flux through the sediments [e.g., *Anderson et al.*, 1979; *Langseth and Herman*, 1981]. Similarly, in sediment-accretionary environments, heat flow can be of great value in the description of the way in which sediments are accreted and pore fluids expelled during deformation [e.g., *Yamano et al.*, 1984].

In all cases, the heat flow must be well characterized, both in plan and with depth. This creates several requirements for the heat flow instrumentation used: (1) Multiple penetrations must be made to characterize local heat flow variations adequately or to verify that none are present and thus that the values measured are regionally representative, (2) thermal conductivity must be measured in situ, for it is rare that both spatial and depth variations in conductivity are small enough for values to be estimated reliably from cored samples, and (3) measurements of in situ temperatures and conductivities must be made in sufficient detail to characterize the conductivity-depth structure and ultimately any depth variations of heat flow that may be present.

Developments in heat flow instrumentation in the past decade have responded well to these needs. Multiple penetration stations were made possible with the instrument design of R. Von Herzen (first described by *Von Herzen and Anderson* [1972]) which used outrigger sensors on a solid strength member to enable many penetrations to be made without mechanical damage to the instrument. A low-resolution acoustic link provided enough data in real time to permit the operator to monitor the status of the instrument during extended stations. A significant improvement to this design was provided by C. Lister (described by *Hyndman et al.* [1978]), who developed a successful high-resolution acoustic telemetry link in order to eliminate the constraint on station duration from data storage capacity and, more importantly, incorporated the solid strength-member design with a single sensor tube which measures both in situ temperatures and thermal conductivities with a closely spaced thermistor array. Many instruments now exist which have followed this "violin bow" design [e.g., *Hyndman et al.*, 1979; *Davis et al.*, 1984; *Hutchison*, 1983], and although differences exist in the details of their design (e.g., thermistor excitation, data acquisition and storage, and telemetry), the problem of the reduction of the massive quantity of data produced by these instruments can be treated in a common way. To deal with this "problem" efficiently yet accurately, we have developed a complete heat flow reduction algorithm that deals with all significant and commonly encountered sources of error and permits in situ temperatures and conductivities to be calculated automatically.

## BACKGROUND

The conductive heat flow through the seafloor is normally determined as the product of the vertical temperature gradient and the thermal conductivity measured with gravity-driven probes or corers in deep-sea sediments. Two methods are commonly used to measure thermal conductivity of deep-sea sediments in situ and in the laboratory. One is a continuously powered line source method [*Von Herzen and Maxwell*, 1959] where the temperature rise of a cylindrical probe is used to calculate the thermal conductivity. The other one is the pulsed line source method [*Lister*, 1979] in which the decay of a calibrated heat pulse is used. Details of the theoretical background of both methods can be found in the work by *Blackwell* [1954] and *Jaeger* [1956]. Historical, constructional, and

[1]Now at Alfred-Wegener-Institut für Polarforschung, Bremerhaven, Federal Republic of Germany.



Paper number 7B6038.
0148-0227/87/007B-6038$05.00

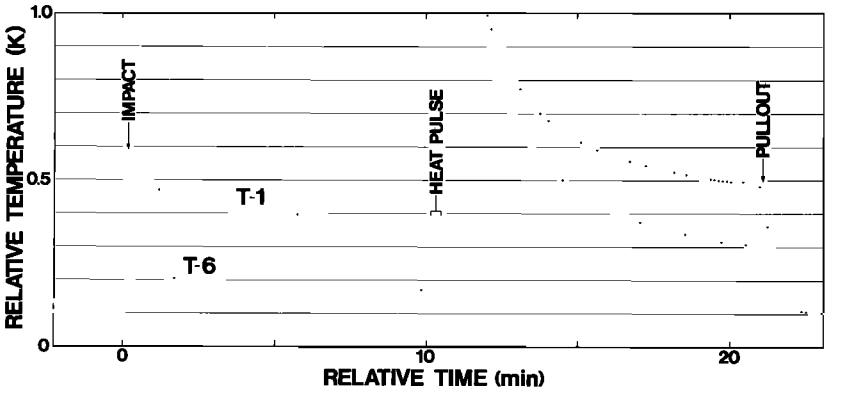


Fig. 1. Record of temperature versus time for a "typical" heat flow measurement. Data for only two sensors are shown for clarity.

operational reasons have led to the exclusive use of the pulsed line source method with violin bow heat flow probes. The lower power required by the pulsed line source method is advantageous for multipenetration heat flow surveys, since with a given battery capacity it allows twice the number of in situ thermal conductivity measurements that is possible with a continuous line source [*Hyndman et al.*, 1979]. With this technique evolving as a standard, we restrict our discussion to problems associated with the reduction of measurements using a violin bow heat flow probe with in situ heat pulse thermal conductivity measurement, although much of the discussion that follows can be applied directly to the reduction of impulse decays obtained with Bullard probes, outrigger sensors, and needle probes and with minor modification to the reduction of continuous line source data as well.

An example of a temperature-time record used for the determination of heat flow is shown in Figure 1. In sequence are (1) the time period prior to final descent and penetration, during which the probe is held some tens of meters above the seafloor and "zero-gradient" reference temperatures are recorded, (2) the frictional heating and subsequent thermal decay following the entry of the probe into the sediments (penetration decay), and (3) the thermal decay following the calibrated heat pulse (heat pulse decay). In brief, the data are reduced in the following way. First, the penetration decay is fitted in a least squares sense with a straight line after its time axis is transformed to the cylindrical decay function $F(\alpha, \tau)$ [*Bullard*, 1954] (see following discussion), with the origin at the time when the impact is first observed. The transformed data are extrapolated to infinite time in order to establish the temperature rise at a given thermistor above the "zero-gradient" reading and to times during the heat pulse decay in order to remove residuals that remain from the penetration disturbance. After these residuals are removed, a conductivity is calculated using the temperature rises above the extrapolated infinite time temperatures measured during the decay following the heat pulse supplied to the sensor string. Use of the cylindrical decay function in both cases requires knowledge of the sediment diffusivity, which is in turn related to the sediment conductivity. Initially, an estimate of the diffusivity is used, and after the conductivity is determined from the heat pulse decay, a second iteration of the reduction is made using a new value of diffusivity determined from the first-computed conductivity and an empirical relationship between diffusivity and conductivity given by *Hyndman et al.* [1979].

## THEORY

The theory for the time-dependent temperature distribution within an infinitely long cylinder subject to a known thermal pulse is presented by *Carslaw and Jaeger* [1959]. Their solution can be applied to the determination of the undisturbed sediment temperature from heat flow probe penetration decays [*Bullard*, 1954] as well as to the in situ measurement of thermal conductivity [*Lister*, 1979]. Assumptions are made that the probe is initially isothermal at a temperature different from that of the sediment and that it is a perfect thermal conductor of known heat capacity per length.

The temperature of the cylinder at a time $t$ is given by

$$T(t) = T_0 F(\alpha, \tau) \tag{1}$$

where

$$F(\alpha, \tau) = \frac{4\alpha}{\pi^2} \int_0^\infty \frac{\exp(-\tau u^2)\, du}{u\, \Delta u} \tag{2}$$

and

$$\Delta u = [uJ_0(u) - \alpha J_1(u)]^2 + [uY_0(u) - \alpha Y_1(u)]^2 \tag{3}$$

$J_n$ and $Y_n$ are Bessel functions of the order $n$ of the first and second kinds, $\tau = (\kappa t)/a^2$ defines the time constant of the cylinder of radius $a$ in a sediment with a thermal diffusivity $\kappa$, and $\alpha$ is twice the ratio of the heat capacity of the sediment to that of the probe material. $T_0$ is the initial temperature of the cylinder above ambient temperature.

For large $\tau$ ($\tau > 10$), $F(\alpha, \tau)$ can be approximated by

$$F(\alpha, \tau) = 1/2\alpha\tau \tag{4}$$

This relationship is best when $\alpha = 2$. Since $T_0$ can be expressed as the total heat input $Q$ divided by the thermal capacity $S$ of the probe and the asymptotic expression for (1) can be written as

$$T(t) = Q/4\pi kt \tag{5}$$

for large $t$. Thus if the heat input is known, either the slope of the measured temperature rise of the cylinder versus $1/t$ or the temperatures at any time during the decay allows us to calculate the thermal conductivity of the sediment:

$$k_{\text{slope}} = \frac{Q}{4\pi}\left[\frac{dT(t)}{d(1/t)}\right]^{-1} \tag{6}$$

or

$$k_{\text{point}} = \frac{Q}{4\pi t T(t)} \tag{7}$$

Relationship (6) or (7) gives a correct value for $k$ only if the large time approximation is valid, i.e., for $\tau > 10$. One way to use (6) or (7) for earlier times is by correcting the temperatures $T(t)$ in such a way that the relationships (6) and (7) are valid for all times [*Lister*, 1979; *Hyndman et al.*, 1979]:

$$T_c(t) = T(t)\, C(\alpha, \tau) \tag{8}$$

with

$$C(\alpha, \tau) = \frac{1}{2\alpha\tau F(\alpha, \tau)} \tag{9}$$

Using (1) with (8) and (9) gives

$$T_c(t) = \frac{T_0}{2\alpha\tau} \tag{10}$$

and replacing $T_0$ with the equivalent heat input yields

$$T_c(t) = \frac{Q}{4\pi k t}$$

which is valid for all times and can be used to calculate the thermal conductivity of the sediment as discussed before.

The calculation of $C(\alpha, \tau)$ requires the knowledge of $\kappa$ and $\alpha$. Simple calculations show that for typical probe constructions $\alpha$ is close to 2 and varies only by about 10% over the thermal conductivity range of deep-sea sediments [*Lister*, 1979; *Hyndman et al.*, 1979]. The thermal diffusivity is obtained from an empirical relationship between thermal conductivity and thermal diffusivity for deep-sea sediments [*Hyndman et al.*, 1979] that was based on the conductivity-water content relationship of *Ratcliff* [1960] and a mean grain specific heat appropriate for red clay and carbonate [*Bullard*, 1954]:

$$\kappa = k/(5.79 - 3.67k + 1.016k^2)10^{-6}\ \text{m}^2\ \text{s}^{-1} \tag{11}$$

This relationship has been confirmed in several environments [e.g., *Hyndman et al.*, 1979; *Davis et al.*, 1984].

With an assumed thermal conductivity $k_{\text{ass}}$, $\kappa$ can be calculated using (11), and under the assumption of $\alpha = 2$ all the needed parameters for $C(\alpha, t)$ are obtained. Thus $T_c(t)$ can be calculated (equations (9) and (2)), and either of the relationships (6) or (7) can be used to compute the conductivity.

## Uncertainties in the Origin Time and Hence a New Reduction Algorithm

Unfortunately, this reduction scheme cannot be used without consideration of another factor that arises from the nonideal nature of heat flow probes. The problem was recognized by *Lister* [1979], who in testing the pulse probe technique noted that "... some phenomenon other than the probe-sediment thermal decay is affecting the results and obvious possibilities are the thermal time constants associated with the internal structure of the sensor string itself." He fitted an exponential function to the nonideal component of the heat pulse decay. In an earlier discussion of probe behavior, *Pratt* [1969] noted that "... the various effects of contact resistance and of temperature sensor position are normally found empirically" and could be accounted for by using a constant time shift of the origin time. This behavior has been observed subsequently by others who have employed the pulse probe measurement technique [*Hyndman et al.*, 1979; *Hutchison*, 1983; *Davis et al.*, 1984].

There are two possible causes of this nonideal behavior: one associated with the nonideal aspects of the probe construction and one associated with the physical disturbance of the sediments due to the penetration of the probe. The internal construction of the sensor string introduces thermal barriers between temperature sensors and the probe's outer surface as well as between internal heater wires and the surface. The filling of the sensor tube with mineral oil helps to reduce these thermal barriers but cannot overcome them completely. These barriers cause a finite thermal response time of the probe and thus a delay both between the time that the heat pulse is delivered by the probe and the time that the heat is received by the surrounding sediment as well as in the times that thermal signals from the sediments appear at the sensors. The magnitude of the composite delay associated with the heat pulse has been obtained by carefully calibrating the sensor string in the laboratory in material with known thermal conductivity. *Hyndman et al.* [1979] and *Mojesky* [1981] found delays that were consistent from test to test with a given sensor but that ranged from about 15 to 30 s depending on the sensor string and on the sensor in a given sensor string used. Our and other's [*Hutchison*, 1983] observations on a number of penetration decays and in situ thermal conductivity measurements with the pulse probe technique suggest that the effective time origin also changes from penetration to penetration. This observation suggests that in the process of penetration the sensor string disturbs the sediment and creates a thin, low thermal conductivity layer at the outside of the sensor tube. This may be caused either by the distortion of the sediments in the direct vicinity of the tube or by a thin layer of water left in the wake of the penetration. If such disturbances are common, then we would expect that (1) a shift of the effective origin time should be present in the penetration as well the heat pulse decay, (2) the distortion of the sediment should decrease with depth, and as a result, so should the shift in the effective origin time, and (3) the shift of the effective origin time should vary with the mechanical characteristics of the sediment. Thus a time delay must be determined individually for each thermistor and each penetration.

To account for the contact resistance and the finite response time of the probe, we have designed ad hoc but physically reasonable procedures to calculate the effective origin times for both the penetration and heat pulse decays. In the case of the penetration decay the appropriate origin time is problematic in two ways. In addition to the unknown delay associated with the various internal and external contact resistances is the uncertain nature of the penetration itself. Penetration in not instantaneous, and the sensor sampling interval is typically too large (e.g., 10 s) for the penetration disturbance to be well characterized. Any inaccuracy in the choice of the penetration time should be reflected in a nonlinearity of the decay temperatures versus $F(\alpha, \tau)$. In the reduction algorithm described here, we use the first indication of the penetration in the temperature record only as the initially assigned origin time. The origin time for each sensor is then shifted by a preset time increment until the standard deviation for the least squares linear fit is minimized. The extrapolated temperature (i.e., for $F(\alpha, \tau) = 0$ at $t = \infty$) is then the undisturbed sediment

temperature at the depth of the sensor. The slope of the penetration decay versus $F(\alpha, \tau)$ is then used to extrapolate the temperature decay to times of the heat pulse decay in order to remove the residual temperature remaining from probe penetration. The success of this technique is apparent in Figure 2*a*, where the scatter in decay values about the best fit line is plotted as a function of effective origin time delay. The minimum in this example occurs at a time substantially later than the time when penetration is first sensed, and the scatter of temperatures about the best fit (0.63 mK) is less than the instrumental resolution (1 mK).

The heat pulse decay appears to behave in much the same way (Figure 2*b*), and a similar criterion is used for determining its effective origin time, although in this case, an additional constraint is applied in the following way. The corrected temperatures of the heat pulse decay $T_c$ versus $1/t$ allow the calculation of a $k_{slope}$ (cf. equation (6)). On the other hand, (7) provides a way of using individual corrected temperatures $T_c$ to determine thermal conductivities $k_{point}$ which should be independent of time. The assumed thermal conductivity $k_{ass}$ is the sought true conductivity of the sediment only if

$$k_{ass} = k_{slope} = k_{point} \tag{12}$$

If (12) is not met within preset error bounds, $k_{ass}$ and the effective origin time are varied, and a new $C(\alpha, \tau)$ function and new $T_c$ values are calculated. Once the condition of (12) is met, the iteration will have converged to a value of $k_{ass}$ where the penetration and heat pulse decays give the same infinite time temperature. In practice, this also occurs where the standard deviation of the linear fit of $T_c$ versus $1/t$ is a minimum.

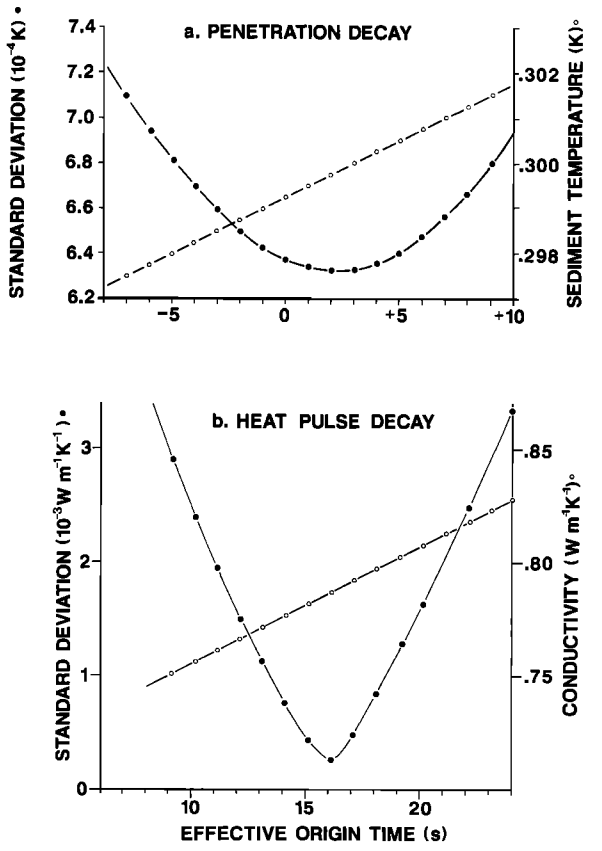


Fig. 2. (*a*) Standard deviation of temperature residuals of the best linear fit to penetration decay temperature versus $F(\alpha, \tau)$ for various values of assumed origin time (solid circles). Open circles show the sediment temperature calculated using the respective origin times. (*b*) Similar plot for the heat pulse decay.

Errors associated with inappropriate origin times can be large (see Figure 3), and as other aspects of the reduction algorithm are relatively straightforward, the remaining discussion focuses primarily on the automatic determination of the effective origin time for the penetration and the heat pulse decays. The complete reduction scheme has been implemented as a Fortran program designed for a microcomputer, and a complete commented version of the program is given by *Villinger and Davis* [1987].

The reduction procedure for the heat pulse decay is illustrated for a single sensor in Figure 3. All the calculations are done in the corrected temperature versus 1/time space using mainly the equations (6), (7), and (10). The procedure starts with an assumed value for $k$ ($k_{ass}$) and an initial estimate of the effective origin time which is shifted by a nominal delay from the center of the heat pulse (Figure 3*a*, line 0). The effective origin time is then varied until $k_{slope}$, the inverse of the slope of the linear least square fit of the corrected temperatures versus 1/time, is equal to $k_{ass}$ (line I). At this stage, $k_{point}$ values and a resultant $k_{point}$ (average) are computed. If $k_{point}$ (average) and $k_{ass}$ differ (i.e., if the $k_{slope}$ fit does not pass through the origin at infinite time), the assumed conductivity $k_{ass}$ is changed and the search for equality of $k_{ass}$ and $k_{slope}$ starts again. The iteration is allowed to terminate if

$$k_{ass} = k_{slope} = k_{point}(\text{average}) \tag{12'}$$

which is the case for line III in Figure 3*a*.

To go from I to II or from II to III in Figure 3*a*, the effective origin time has to be iteratively changed. Figure 3*b* illustrates this procedure. We start out with point I-1 and change the effective origin time by a small amount. A new $k_{slope}$ is calculated (point I-2) that is farther from or closer to $k_{ass}$ than the original value. With the trend known, a third origin time is determined and used to calculate a third $k_{slope}$ (point I-3). The size of the iteration steps is calculated with the method of false position (Regula Falsi). The iteration continues until point I-4 is reached for which the $\Delta k$ is within a preset error bound. We then compute $k_{point}$(average), change $k_{ass}$ to be equal to $k_{point}$(average), and come, with the same effective origin time, to point II-1. The same procedure is then repeated. At the point III-3 the assumed thermal conductivity, the slope conductivity, and the mean of the point thermal conductivities are equal, and therefore the true value for the sediment thermal conductivity is found. Although linearity of the decay is not used explicitly as a constraint in determining the best origin time as is the case with the penetration decays, the final solution (point III-3) usually coincides with a minimal standard deviation of the residuals when fitting $T_c$ versus $1/t$ as expected (Figures 3*c* and 2*b*).

The two iteration loops explained above are required to find the true thermal conductivity of the sediment. In the "inner loop" the assumed thermal conductivity is kept fixed and the time shift is iteratively changed until

$$k_{ass} = k_{slope}$$

within a preset error bound $k_{toler}$, i.e., until

$$\Delta k = |k_{ass} - k_{slope}| \leq k_{toler}$$

In the "outer loop," $k_{ass}$ is varied until the intercept temper-

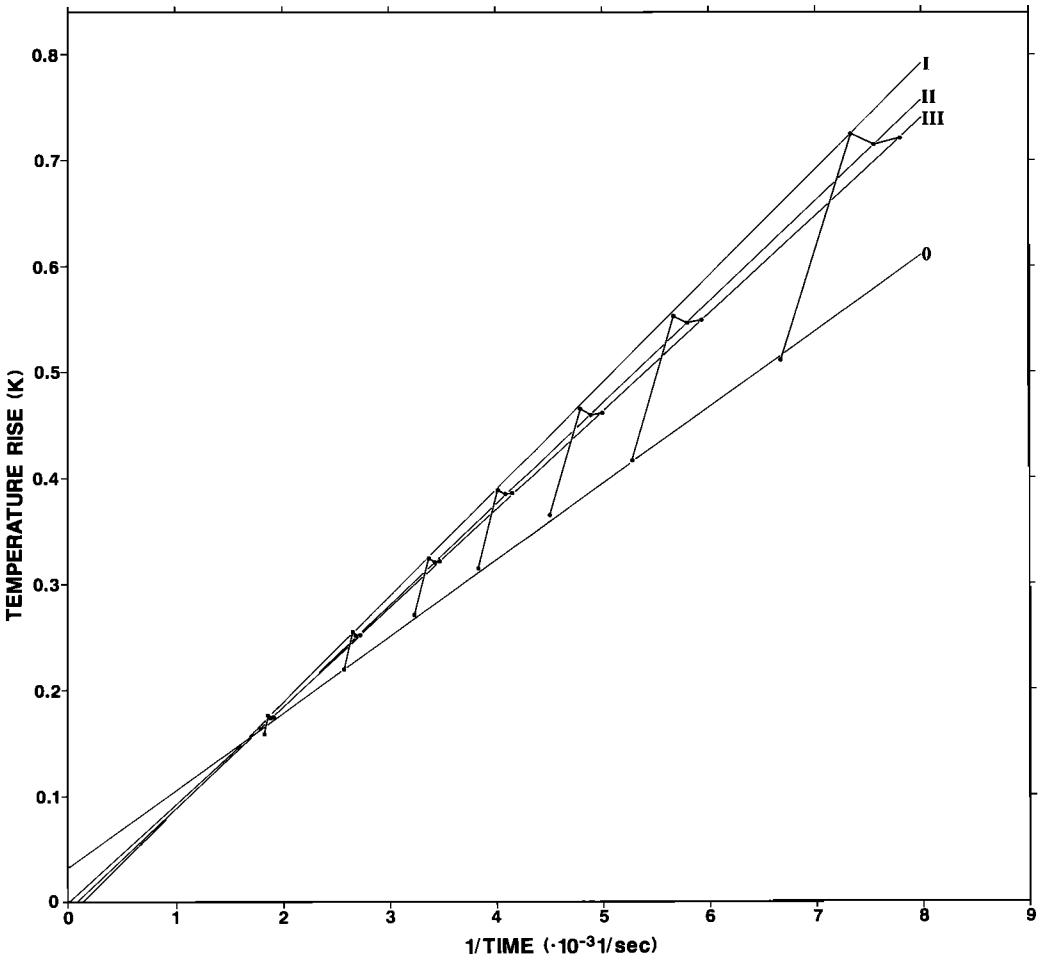


Fig. 3*a*. Example of temperature versus 1/time of a heat pulse decay at various stages of the reduction process. Points along the best fitting line 0 are measured temperature-time points. Points along I and II are corrected temperatures $T_c$ plotted against $1/t$ after a time shift has been applied to make $k_{ass} = k_{slope}$. The line through the final points of the final iteration, III, passes through the origin and satisfies the equality $k_{ass} = k_{slope} = k_{point}$(average).

ature for $t = \infty$ is zero (cf. Figure 3*a*), which occurs when

$$k_{point}(\text{average}) = k_{slope}$$

to the same level of agreement $k_{toler}$.

In the complete heat flow reduction algorithm, this outer loop includes the penetration decay calculation, as the penetration decay fit and thus the decay residuals and the equilibrium temperatures are affected by the assumed conductivities. Experience shows that after two cycles the results remain unchanged and vary only at the noise level of the input data.

## Tests for Sensitivity to Reduction Parameters

A number of numerical tests have been made to determine the sensitivity of the algorithm to the reduction parameters. These are (1) the error bound $k_{toler}$ in the iteration loops, (2) the chosen value value of $\alpha$, and (3) the initially assumed thermal conductivity $k_{ass}$.

The error bound $k_{toler}$ controls both the "inner" and "outer" iteration loops and thus the total number of iterations since it is the criterion for their termination. It is therefore necessary to investigate the influence of this value on the final $k$. Using a number of penetrations, $k$ was calculated for various values of $k_{toler}$ which increased from 0.0001 to 0.005 W m$^{-1}$ K$^{-1}$. The resulting conductivities were compared to the results obtained with $k_{toler} = 0.0001$ W m$^{-1}$ K$^{-1}$; differences are plotted as frequency histograms in Figure 4. A value of $k_{toler}$ of about 0.001 W m$^{-1}$ K$^{-1}$ appears to be an optimal value, in that it guarantees correct results with a minimum of iterations.

The ratio of the thermal capacities of the sediment and the probe varies with changing sediment properties. Under the assumption of (11) this results in

$$\alpha = \frac{2\pi a^2(5.79 - 3.67k + 1.016k^2)}{S} \tag{13}$$

with $S = 2\pi a^2 \rho C$ (probe) being the thermal capacity per unit length of the probe itself. Ideally, this variation should be accounted for. In practice, however, the effect is small. Values of $\rho C$ have been estimated by *Lister* [1979] and *Hyndman et al.* [1979] for typical probe constructions. Using $\rho C = 3.3 \times 10^6$ J m$^{-3}$ K$^{-1}$, (13) can be calculated for arbitrary $\alpha$ or $k$ values. The resulting function is shown in Figure 5*a* (circled points). We have reduced several penetrations using varying values of $\alpha$ ranging from 1.8 to 2.2. Results are also shown in Figure 5*a*. Over this range of conductivity, the error introduced by assuming $\alpha = 2$ is $\leq 1\%$. With such insensitivity of $k$ to $\alpha$, it is adequate to use a fixed value of 2.0 for most sediments. If extreme conductivities are encountered, a correc-

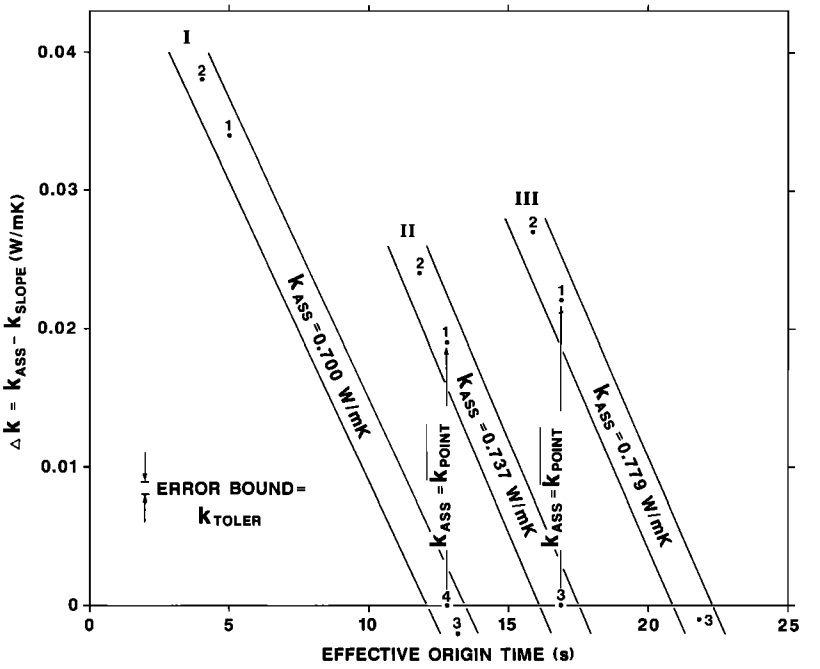


Fig. 3*b*. The difference between $k_{ass}$ and $k_{slope}$ as a function of effective origin time and assumed thermal conductivity $k_{ass}$. The path of the iteration process can be traced from point to point, with the Roman and Arabic numerals corresponding to the outer and inner loops of the reduction algorithm.

tion factor can be used to compensate for the use of an incorrect $\alpha$ value (Figure 5*b*).

Sensitivity to the choice of the initially used $k_{ass}$ is demonstrated in Figure 6. Clearly the choice is not crucial for the reduction algorithm as long as it is within reasonable limits of deep-sea sediment thermal conductivities. The same test of the reduction algorithm was performed by using model input data calculated with a known thermal conductivity. Resulting calculated $k$ values were always within 0.2% of the assumed model thermal conductivity.

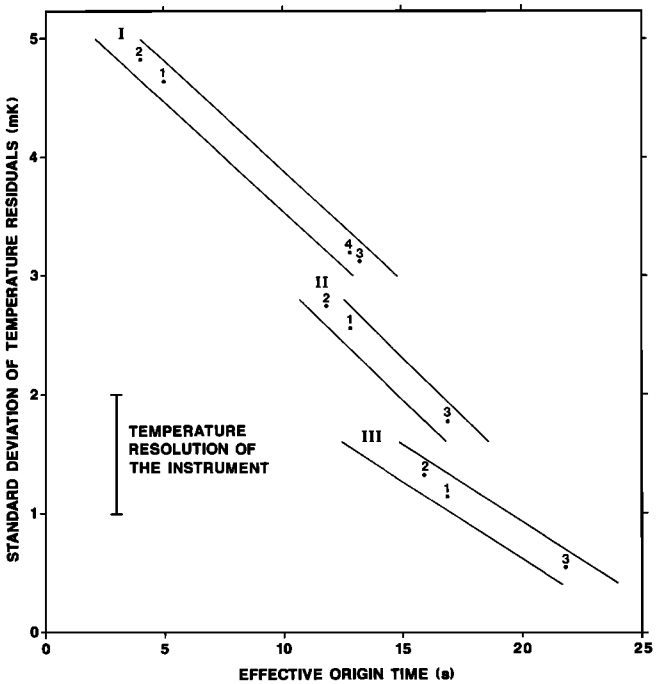


Fig. 3*c*. The standard deviation of the residuals of the linear fit of $T_c$ versus 1/time (cf. Figure 3*a*) for various stages of the reduction algorithm. Correspondence of the best fit with the final solution at $k_{ass} = k_{slope} = k_{point}$ (average) (point III-3) provides an excellent internal consistency check of the algorithm.

The use of a finite length heat pulse has been vindicated on theoretical grounds by *Lister* [1979] and in practice through calibration of probes having a variety of diameters and pulse lengths [*Hyndman et al.*, 1979; *Mojesky*, 1981; H. Villinger, personal communication, 1987]. In an extreme case the decay of a 1-mm needle probe having a pulse length of 10 s conformed to theory in spite of the ratio of the probes thermal time constant to the pulse length being only about 2:1.

## PRACTICAL TESTS OF THE ALGORITHM

We have used the described algorithm for the reduction of about 100 heat flow measurements made during a cruise in the western Pacific (TGT-178; for details see C. R. B. Lister et al. (manuscript in preparation, 1987)). The probe used was designed by C. R. B. Lister from the University of Washington (Seattle) and is described in detail by *Davis et al.* [1984]. This first application of the reduction algorithm was an excellent performance test for the program as the data quality is particularly and consistently high. The results allow us to examine our assumptions and perceptions about the causes of nonideal behavior of the frictional and heat pulse decays.

Figure 7 shows a typical example of the reduction of a penetration decay. A number of things are noteworthy: The best fit of temperatures versus $F(\alpha, t)$ occurs for an assumed origin time that is significantly later than the moment of penetration defined by the first observed temperature rise (see Figure 2*a*). In this case the origin time that provides the best fit is fairly well defined, but this definition is dependent on the slope of the temperature versus $F(\alpha, \tau)$ decay. Lack of convergence may occur for low slopes; these are dealt with in the

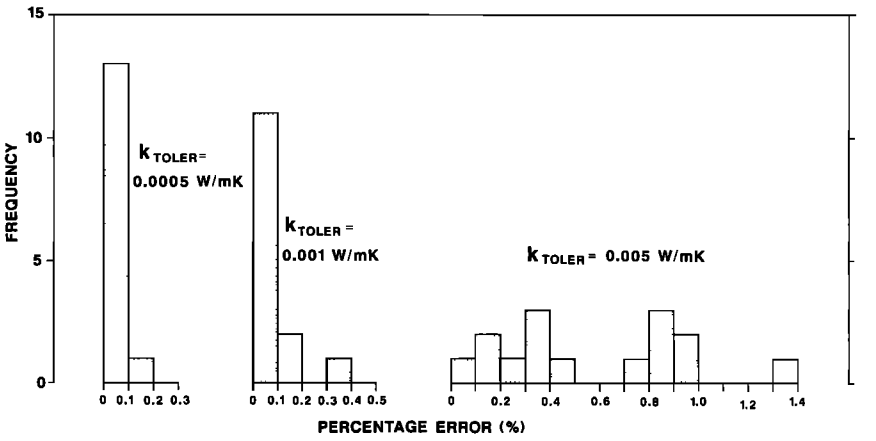


Fig. 4. Frequency distribution of percentage errors due to a particular choice of $k_{toler}$.

reduction scheme by limiting the possible range of the time shift. The sediment temperature at the estimated infinite time intercept is relatively insensitive to the choice of the origin time, particularly at low slope, as are the residuals removed from the heat pulse decay. Including this step in the reduction process does, however, improve the ultimate accuracy of both the gradient and the conductivity determinations. It also provides a flag for the recognition of disturbed penetration decays, and it is interesting to note that including the adjustment of penetration time increases the convergence speed of the heat pulse decay calculations.

The effective origin times for the penetration decays of all sensors are generally between +10 and −10 s (Figure 8*a*). The scatter in effective origin times is quite large and probably due to the very broad minima determined for many of the decays which have low slopes. Variation of origin time with depth is consistent with the nature of penetration: bottom sensors first. There is not obvious explanation for the abrupt change in effective origin time between sensor 3 and 4.

Figure 8*b* shows the effective origin times for the heat pulse decays as a function of sensor (and depth). The reduction algorithm gives very consistent effective origin times for each sensor. They do not vary from penetration to penetration by more than 15% for each of the sensors 1 to 6. The magnitude of the effective origin time calculated with the program agrees very well with other estimates for probes of similar construction [*Hyndman et al.*, 1979; *Mojesky*, 1981; *Hutchison*, 1983; *Davis et al.*, 1984]. There is a substantial variation with depth, however; the average origin time delays increase from about 15 s (sensor 1) to about 25 s (sensor 6). This systematic variation is believed to be due to the increase in the amount of sediment disturbance up the probe from sensor 1 to sensor 7, along with the changing probe properties along the length of the probe due to the greater number of wires and perhaps

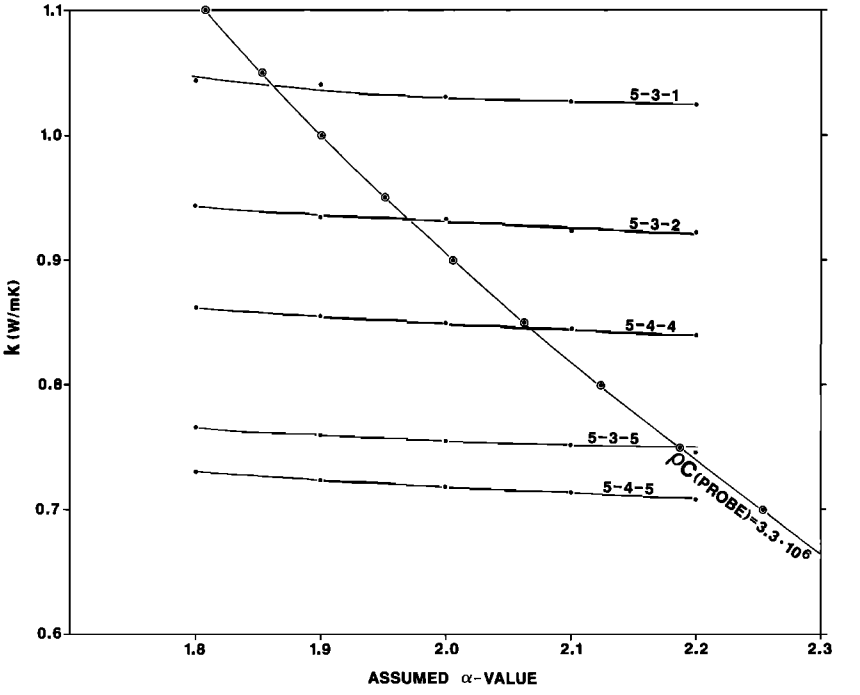


Fig. 5*a*. The influence of the $\alpha$ value used in the reduction algorithm on the final thermal conductivity shown for various penetrations and sensors of station 5, TGT-178. The dashed curve was calculated using equation (13) and under the assumption of a thermal capacity of the probe of $3.3 \times 10^6$ J m$^{-3}$ K$^{-1}$.

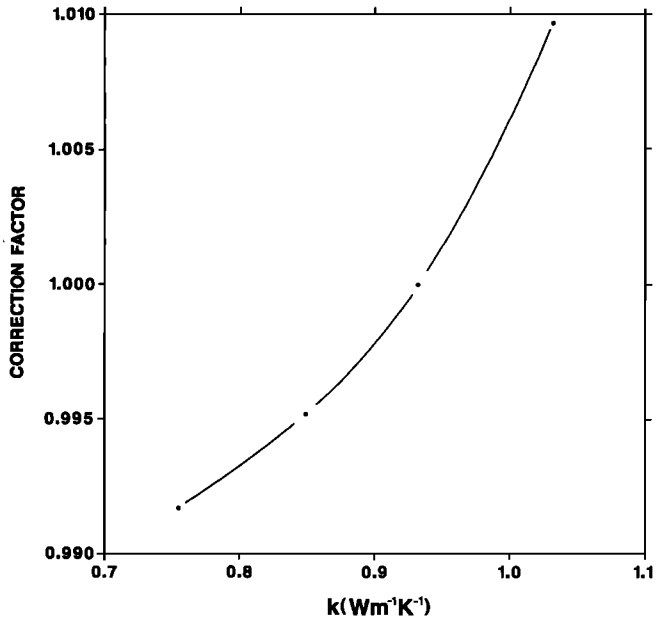


Fig. 5b. Conductivity correction factor to account for the error in assuming $\alpha = 2$, calculated using results from Figure 5a and plotted as a function of thermal conductivity.

incomplete oil fill in the upper portion of the sensor string. Results from different sites demonstrate that the effective origin time is not resolvably dependent on the thermal conductivity (see Figure 9). This does not imply lack of dependence of time delay on mechanical properties of the sediment, however, since in this case the variability of conductivity is as much due to variations in carbonate content as it is to variations in porosity (C. R. B. Lister et al., manuscript in preparation, 1987). The data for sensor 7 are in many cases more disturbed due to occasional superpenetration of the weight stand. Results for the uppermost sensor should therefore be regarded with caution.

A very good consistency check for the algorithm is provided by the equation

$$T(t) = T_0 F(\alpha, \tau) \tag{14}$$

where in the case of an ideal probe $T_0$ is the initial temperature at $t = 0$. In theory this value should be constant for a specific probe

$$T_0 = Q/S = \text{const} \tag{15}$$

as $Q$ and $S$ depend only on probe parameters. For the probe used, $S$ is estimated as $3.3 \times 10^6$ J m$^{-3}$ K$^{-1}$, and $Q$ is measured to be 906 J m$^{-1}$. These values would yield a $T_0$ of 3.86 K. $T_0$ can also be calculated from the data since

$$T_0 = \frac{\alpha Q}{[(2\pi a^2) * (5.79 - 3.67k + 1.016k^2]} \times 10^{-6} \tag{16}$$

If alpha varies, $T_0$ should remain constant as it does not depend on sediment properties. However, in our reduction scheme alpha is kept fixed for varying values of $k$ in (14), and as a result, $T_0$ effectively varies with changing $k$ according to (16). This function and all the determined $T_0$ values are shown in Figure 10. The agreement is extremely good. Scatter might be due to scatter in $Q$ and/or general "reduction noise."

A final test of the reduction algorithm consisted of a comparison of heat flow reductions of data collected with a variety of other instruments. The violin bow instruments used at Pacific Geoscience Centre (Sidney, British Columbia), at Memorial University (St. John's, Newfoundland), and at Dalhousie University (Halifax, Nova Scotia) all have different internal probe constructions, temperature resolutions, and heat pulse strength. Reduction of data sets from all of these probes confirmed the agorithm's performance and suggested that the re-

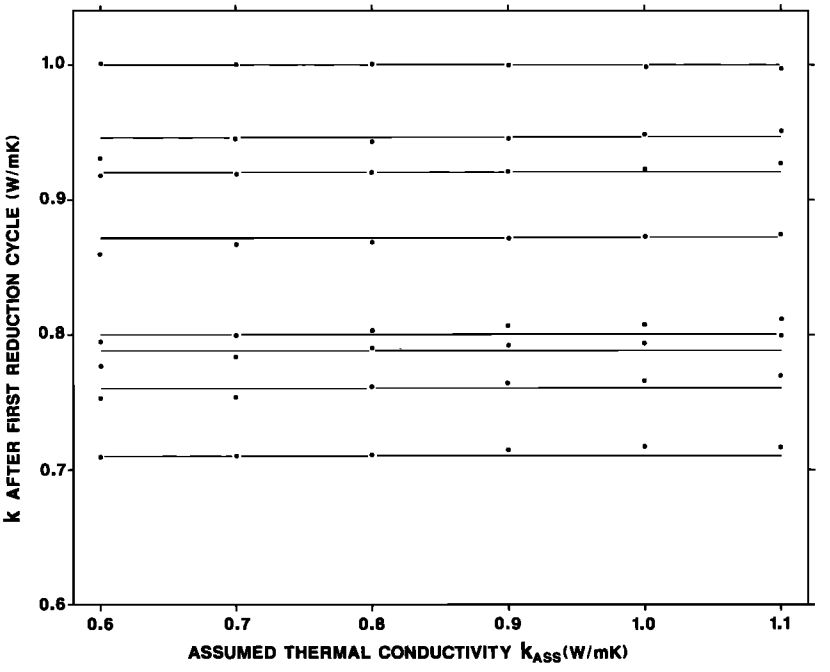


Fig. 6. The effect of the initially assumed thermal conductivity $k_{ass}$ on the results after the first reduction cycle, determined for measurements in sediments of the western Pacific (cruise TGT-178) having a wide range of thermal conductivities. Final values of conductivity calculated after a second iteration are shown as horizontal lines.

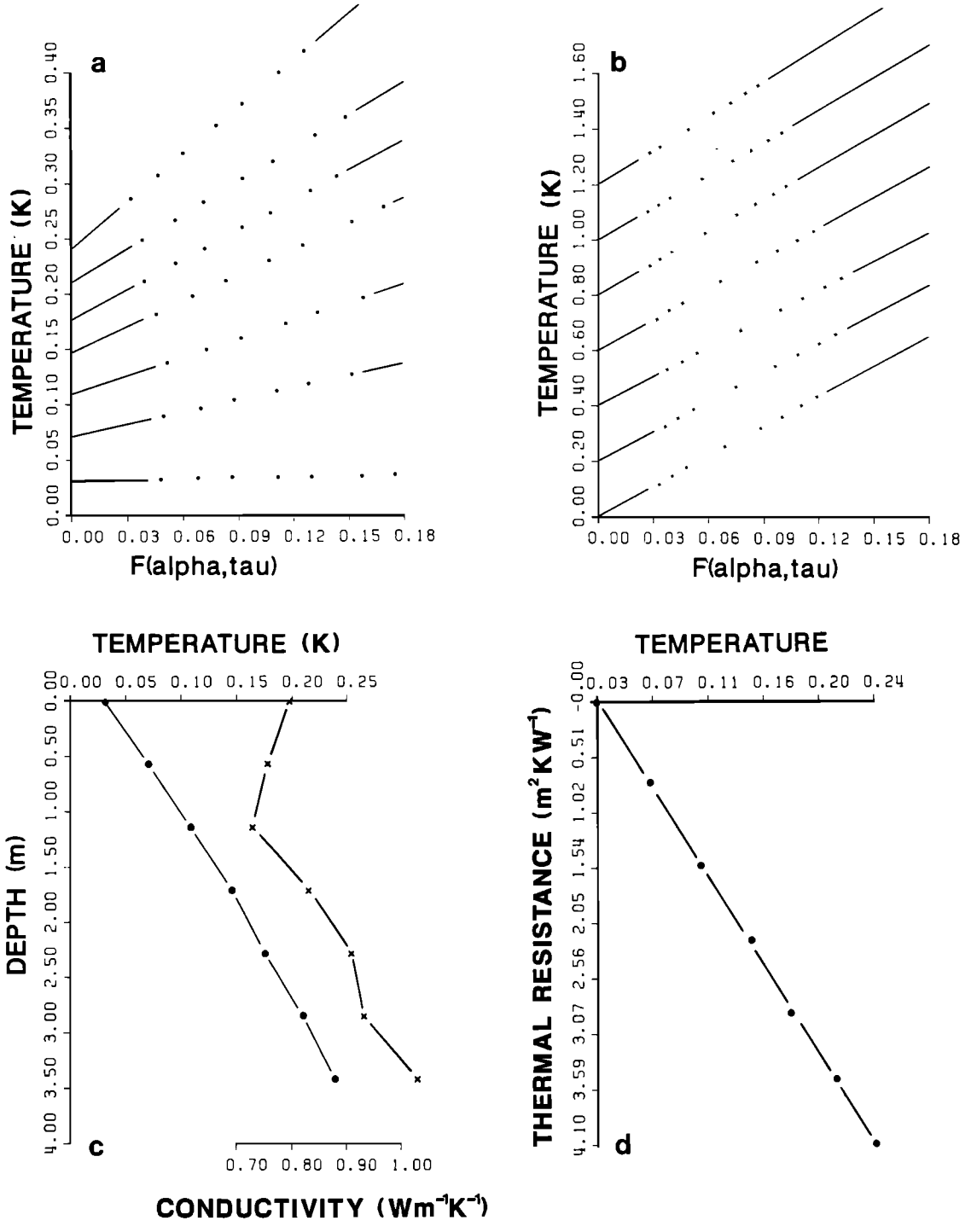


Fig. 7. Results of a typical heat flow penetration, showing the plots of the (*a*) penetration and (*b*) heat pulse decays after two iterations of the reduction algorithm, and the resultant (*c*) temperature and conductivity versus depth and (*d*) temperature versus thermal resistance.

duction of the TGT-178 data set described in this paper is typical.

## SUMMARY

A new scheme has been presented for the reduction of marine heat flow data. The scheme has been developed specifically for instruments employing the pulsed line source method of in situ conductivity measurement, although most of the problems dealt with in the reduction algorithm are common to those encountered using the continuous line source method as well.

The theory used to describe the temperature rise or decay following probe penetration and the temperature decay following a calibrated heat pulse is that for a perfectly conductive cylinder imbedded in a medium of uniform thermal conductivity. However, the theory is not entirely suitable for several reasons: (1) Typical probe constructions are not ideal. Low conductivity paths are present between the line source of

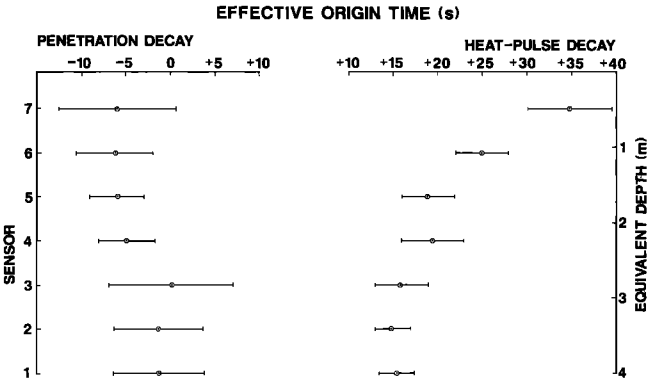


Fig. 8. The effective origin time of the penetration and heat pulse decays plotted against sensor depth for all penetrations of cruise TGT-178. The standard deviations for each sensor are indicated.

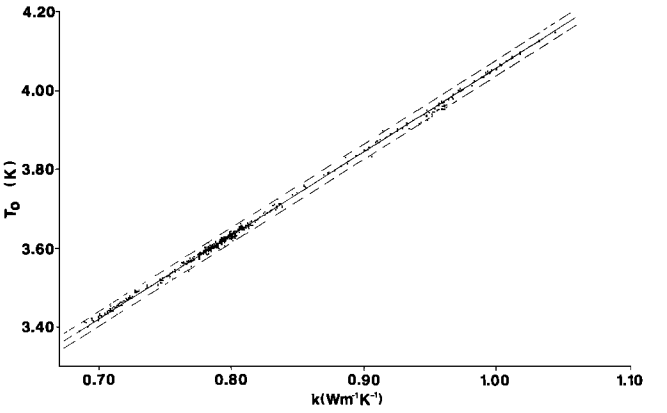


Fig. 10. The slope $T_0$ as a function of thermal conductivity for all penetrations and sensors of TGT-178. The solid line was calculated with (13). The dashed lines indicate a 10% error margin.

heat and the steel wall of the probe, and between the probe wall and the thermistor sensors. (2) Penetration of the probe into the seafloor disturbs the sediments, producing a thermal barrier between the probe and the undisturbed sediments. (3) Probe penetration is not instantaneous. In the reduction scheme, these nonideal conditions are assumed to produce a composite time delay between the times that the heat is generated and the times the thermal signal in the sediments is sensed. Selection of the appropriate time delay is made on a sensor by sensor basis for each penetration. The effective origin time of penetration is determined by requiring that the penetration decays follow a linear $F(\alpha, \tau)$ relationship as predicted by ideal probe theory. A similar criterion is applied to the heat pulse decay, although in this case, two independent constraints are available: (1) the decay of temperature must be linear in an $F(\alpha, \tau)$ sense, and (2) the infinite time ($F(\alpha, \tau) = 0$) intercept must be equal to the equilibrium temperature determined by the extrapolation of the penetration decay.

The use of an effective origin time delay in the analysis of line source data is physically reasonable, but nevertheless ad hoc. However, numerical simulations of a nonideal probe [*Hyndman et al.*, 1979] produced comparable time shifts to those found in our data reductions. Furthermore, tests of the reduction algorithm on a particularly high-quality data set

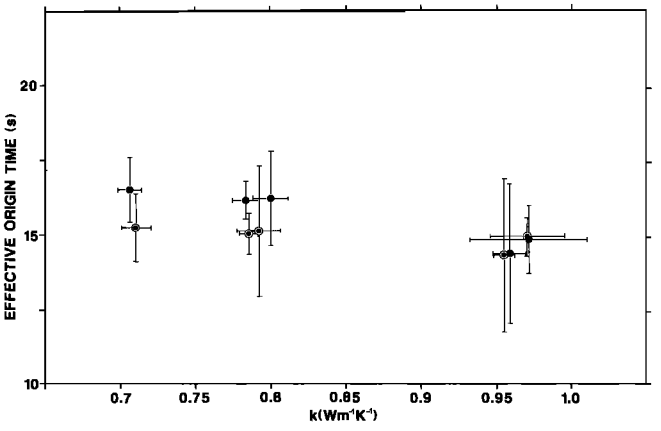


Fig. 9. The effective origin time delay of the heat pulse decay as a function of conductivity for approximately 100 measurements at four sites in the western Pacific (cruise TGT-178). Only values determined using the lowermost two sensors (solid and circled points) are shown to avoid the sensitivity of the origin time to sensor depth (see Figure 8). Conductivities at each site are extremely uniform.

produced the following results: (1) The standard deviation of residuals between temperatures and best fitting (delayed) $F(\alpha, \tau)$ lines are always at or below the level of instrumental resolution (1 mK), for both penetration and heat pulse decays. These residual minima are well defined and single-valued (Figure 2). (2) In the case of the heat pluse decays, the residual minima occur at an effective origin time that also satisfies the criterion that the infinite-time intercept is equal to that determined from the frictional decay (Figure 3). (3) The best fitting time delays yield initial temperature rises (predicted by the slope of the $F(\alpha, \tau)$ heat pulse decay curve) that are independent of conductivity, as required by theory. Finally, the use of a time delay has been checked by full instrumental and data reduction calibration in materials of known or otherwise determined conductivity [*Hyndman et al.*, 1979; *Mojesky*, 1981; *Davis*, 1987].

Accounting for nonideal probe behavior is necessary to obtain accurate in situ temperatures and conductivities. For the examples shown in Figures 3*a* and 3*b*, 10-s errors in the penetration or heat pulse origin times result in errors of 3 mK and 0.05 W $m^{-1}$ $K^{-1}$ in temperature and conductivity, respectively. Such errors would lead to substantial (10–20%) errors in interval heat flow values computed for typical thermistor arrays used in marine studies. With the use of the algorithm described here, and full instrument calibration, one can now determine the undisturbed sediment temperature to better than 1 mK and the in situ thermal conductivity to within 1%. This ability to measure marine heat flow to a higher resolution than was previously possible has important consequences for future studies of heat and fluid transfer through the lithosphere, crust, and sediments of ocean ridges, basins, and margins.

*Acknowledgments.* The authors thank J. Wright (Memorial University) and K. Louden (Dalhousie University) for the use of their data for testing the reduction algorithm. The primary data set used for the tests were collected on cruise 178 of the T. G. Thompson (University of Washington) for which C. Lister was chief scientist. H. Villinger was supported by an NSERC research fellowship. Helpful comments were provided by D. Chapman. Geological Survey of Canada contribution 21487.

## REFERENCES

Anderson, R. N., M. A. Hobart, and M. G. Langseth, Geothermal convection through oceanic crust and sediments in the Indian Ocean, *Science*, *204*, 828–832, 1979.

Blackwell, J. H., A transient flow method for determination of ther-

mal constants of insulating materials in bulk, *J. Appl. Phys.*, *25*, 137–144, 1954.

Bullard, E. C., Heat flow in South Africa, *Proc. R. Soc. London, Ser. A*, *173*, 474–502, 1939.

Bullard, E. C., The flow of heat through the floor of the Atlantic Ocean, *Proc. R. Soc. London, Ser. A*, *222*, 408–429, 1954.

Carslaw, H. S., and J. C. Jaeger, *Conduction of Heat in Solids*, 2nd ed., Oxford University Press, London, 1959.

Courtney, R. C., and R. S. White, Anomalous heat flow and geoid across the Cape Verde Rise: Evidence for dynamic support from a thermal plume in the mantle, *Geophys. J. R. Astron. Soc.*, *87*, 815–867, 1986.

Davis, E. E., Determining heat flow through marine sediments, in *Handbook for Terrestrial Heat-Flow Density Determination*, edited by R. Heaenel, L. Ryback, and L. Stegena, D. Reidel, Hingham, Mass., in press, 1987.

Davis, E. E., C. R. B. Lister, and J. G. Sclater, Towards determining the thermal state of old ocean lithosphere: Heat-flow measurements from the Blake-Bahama outer ridge, northwestern Atlantic, *Geophys. J. R. Astron. Soc.*, *78*, 507–545, 1984.

Detrick, R. S., R. P. Von Herzen, B. Parsons, D. Sandwell, and M. Doherty, Heat flow observations on the Bermuda Rise and thermal models of mid-plate swells, *J. Geophys. Res.*, *91*, 3701–3723, 1986.

Green, K. E., R. P. Von Herzen, and D. L. Williams, The Galapagos spreading center at 86°W: A detailed geothermal field study, *J. Geophys. Res.*, *86*, 979–986, 1981.

Hutchison, I., Heat flow studies in the Gulf of Oman and western Mediterranean, Ph.D. thesis, Univ. of Cambridge, Cambridge, 1983.

Hyndman, R. D., G. C. Rogers, M. N. Bone, C. R. B. Lister, U. S. Wade, D. L. Barrett, E. E. Davis, T. Lewis, S. Lynch, and D. Seemann, Geophysical measurements in the region of the Explorer ridge off western Canada, *Can. J. Earth Sci.*, *15*, 1508–1525, 1978.

Hyndman, R. D., E. E. Davis, and J. A. Wright, The measurement of marine geothermal heat flow by a multipenetration probe with digital acoustic telemetry and in situ thermal conductivity, *Mar. Geophys. Res.*, *4*, 181–205, 1979.

Jaeger, J. C., Conduction of heat in an infinite region bounded internally by a circular cylinder of a perfect conductor, *Aust. J. Phys.*, *9*, 167–179, 1956.

Langseth, M. G., and B. M. Herman, Heat transfer in the oceanic crust of the Brazil Basin, *J. Geophys. Res.*, *86*, 10,805–10,819, 1981.

Langseth, M. G., M. A. Hobart, and K. Horai, Heat flow in the Bering Sea, *J. Geophys. Res.*, *85*, 3740–3750, 1980.

Lister, C. R. B., The pulse-probe method of conductivity measurement, *Geophys. J. R. Astron. Soc.*, *57*, 451–461, 1979.

Louden, K. E., D. O. Wallace, and R. C. Courtney, Heat flow and depth versus age for the Mesozoic N.W. Atlantic Ocean: Results from the Sohm abyssal plain and implications for the Bermuda Rise, *Earth Planet. Sci. Lett.*, in press, 1987.

Mojesky, T., Rapid in situ thermal conductivity measurements for the study of geothermal heat flow, M.S. thesis, Univ. of Wash., Seattle, 1981.

Pratt, A. W., Heat transmission in low conductivity materials, in *Thermal Conductivity*, edited by R. P. Tye, pp. 301–402, Academic, Orlando, Fla., 1969.

Ratcliff, E. H., Thermal conductivities of ocean sediments, *J. Geophys. Res.*, *65*, 1535–1541, 1960.

Tamaki, K., Age of the Japan Sea, *J. Geogr.*, *94*, 14–29, 1985.

Villinger, H., and E. E. Davis, HFRED: A program for the reduction of marine heat-flow data on a microcomputer, *Geol. Sur. Can Open File Rep.*, *1627*, 1987.

Von Herzen, R. P., and R. N. Anderson, Implications of heat flow and bottom water temperature in the eastern equatorial Pacific, *Geophys. J. R. Astron. Soc.*, *26*, 427–458, 1972.

Von Herzen, R. P., and A. E. Maxwell, The measurement of thermal conductivity of deep-sea sediments by a needle probe method, *J. Geophys. Res.*, *64*, 1557–1563, 1959.

Von Herzen, R. P., R. S. Detrick, S. T. Crough, D. Epp, and U. Fehn, Thermal origin of the Hawaiian swell: Heat flow evidence and thermal models, *J. Geophys. Res.*, *87*, 6711–6723, 1982.

Yamano, M.,S. Honda, and S. Uyeda, Nankai Trough: A hot trench?, *Mar. Geophys. Res.*, *6*, 187–203, 1984.

E. E. Davis, Pacific Geoscience Centre, Energy, Mines and Resources, 9860 West Saanich Road, P.O. Box 6000, Sidney, B.C., Canada V8L 4B2.

H. Villinger, Alfred-Wegener-Institut für Polarforschung, D-2850 Bremerhaven, Federal Republic of Germany.

(Received March 17, 1987;
revised July 15, 1987;
accepted August 10, 1987.)